Stress in a dilute suspension of spheres in a dilute polymer solution subject to simple shear flow at finite Deborah numbers

Donald L. Koch* and Eric F. Lee
School of Chemical and Biomolecular Engineering, Cornell University, Ithaca, New York 14853, USA

Ibrahim Mustafa
Department of Chemical Engineering Technology, Yanbu Industrial College, Yanbu, Kingdom of Saudi Arabia
(Received 17 January 2016; published 2 May 2016)

The influence of particle-polymer interactions on the ensemble average stress is derived as a function of the Deborah number for a dilute suspension of spheres in an Oldroyd-B fluid in the limit of small polymer concentrations. The slow rate of decay of the particle-induced polymer stress with separation from a particle presents a challenge to the derivation of the average stress, which can be overcome by removing the linearized polymer stress disturbance before computing the bulk average stress from the particle-induced disturbance. The linearized stress can be shown to have zero ensemble average. The polymer influence on the particle's stresslet is computed with the aid of a generalized reciprocal theorem based on a regular perturbation from Newtonian flow for small polymer concentration. The analysis shows that the particle-polymer contributions to the shear stress and first normal stress difference shear thicken as has been observed in the experiments of Scirocco *et al.* [Shear thickening in filled Boger fluids, J. Rheol. **49**, 551 (2005)]. The particle-polymer contribution to the second normal stress difference is positive at small Deborah numbers but changes sign at a Deborah number of about 2.3.

DOI: 10.1103/PhysRevFluids.1.013301

I. INTRODUCTION

The rheology of particle suspensions in polymeric fluids is important in many applications including injection molding of composite materials and the design of paints, coatings, health care, and food products. Many experimental studies [1–7] and limited multiparticle simulations [8–10] have explored the rheology of particle-filled polymeric fluids. The stress in a particle-polymer suspension is influenced by the particle stresslet, representing the stress transmitted through the interior of the rigid particles, and by the stresses caused by the deformed polymers. The fluid velocity disturbances induced by the particles alter the polymeric stresses. The particle stresslets in turn are affected by the polymer stresses and by the modification of the fluid velocity and pressure fields due to the polymer rheology. A theoretical problem that captures both of these couplings in the absence of particle-particle interactions is the determination of the ensemble average stress in a dilute suspension of particles that are assumed to be well dispersed. The only existing theoretical studies of this kind [11–13] have considered the low-Deborah-number limit $\mathrm{De} = \lambda\dot{\gamma} \ll 1$, in which the second-order fluid rheological equation is applicable. Here $\dot{\gamma}$ is the shear rate, λ is the polymer relaxation time, and the Deborah number is defined as the ratio of the particle relaxation time to the $\dot{\gamma}^{-1}$ time scale of a polymer-particle encounter. In the present study, we provide a theoretical treatment of the shear-rate dependence of the rheology of a particle-polymer suspension by considering the rheology of a dilute suspension of spherical particles in a polymer solution that follows the Oldroyd-B constitutive equation. A quasianalytical treatment is facilitated by considering the limit of small dimensionless polymer concentration $c \ll 1$. Here c is defined as the number of polymers per unit volume times the cube of the radius of gyration. By computing the particle stresslet and the extra polymer stress

*dlk15@cornell.edu

due to particle disturbances, we will determine the shear-rate dependence of the viscosity and the first and second normal stress coefficients. We characterize this shear-rate dependence in terms of the Deborah number defined above rather than a Weissenberg number, because it is the changes in polymer behavior as the time scale of polymer-particle encounter decreases that leads to modification of the stress. The elastic stresses and associated flow modification (measured by the Weissenberg number) remain small in the limit $c \ll 1$.

The determination of the stress in a suspension of particles in the limit of small particle volume fraction ϕ provides a natural starting point for understanding the rheology of a suspension. Einstein [14] showed that a dilute suspension of spherical particles in a Newtonian fluid enhances the effective viscosity μ of a suspension so that $\mu = \mu^s(1 + \frac{5}{2}\phi)$, where μ^s is the viscosity of the fluid. Koch and Subramanian [11] used an ensemble averaged equation approach [15] to derive the stress in a dilute suspension of spheres in a second-order fluid. Up to $O(\mathrm{De})$, the shear stress of the suspension, like that of the fluid, is unaltered from its Newtonian value. The normal stresses in the suspension are quadratic functions of the shear rate, so

$$N_1 = \langle\sigma_{11}\rangle - \langle\sigma_{22}\rangle = \psi_1\dot{\gamma}^2 \tag{1}$$

and

$$N_2 = \langle\sigma_{22}\rangle - \langle\sigma_{33}\rangle = \psi_2\dot{\gamma}^2, \tag{2}$$

where the imposed fluid velocity is $\langle\mathbf{u}\rangle = \dot{\gamma}\mathbf{e}_1 r_2$. Here the angular brackets indicate an ensemble average, $\boldsymbol{\sigma}$ is the stress, $\mathbf{e}_1$ is a unit vector, and $\mathbf{r}$ is the position. Koch and Subramanian showed that the normal stress coefficients ψ_1 and ψ_2 of the suspension are related to those ψ_1^f and ψ_2^f of the suspending fluid by $\psi_1 = \psi_1^f(1 + \frac{5}{2}\phi)$ and $\psi_2 = \psi_2^f + \frac{75}{28}\phi\psi_2^f + \frac{5}{56}\phi\psi_1^f$. Thus, the particles enhance the first normal stress coefficient by the same factor as the viscosity. The particle effect on the second normal stress coefficient is more complex. It is negative for most polymeric fluids [16], for which $\psi_2^f < 0$ and $|\psi_2^f| = 0.05 - 0.3\psi_1^f$, but positive for an Oldroyd-B fluid, for which $\psi_2^f = 0$. In evaluating the effect of the alteration of the fluid velocity and pressure on the particle stresslet, Koch and Subramanian took two alternative approaches, one of which involved the use of the $O(\mathrm{De})$ perturbation to the velocity and pressure that had been derived by Peery [17], while the second avoided the need for this non-Newtonian flow solution by invoking a generalized reciprocal theorem. The two approaches gave the same results. Greco *et al.* [18] and Housiadas and Tanner [19] adopted a volume average approach and used the $O(\mathrm{De})$ perturbation to the flow field. They confirmed Koch and Subramanian's result for the particle stresslet, but they argued incorrectly that the effect of the particles on the average polymer stress was zero. Subsequently, Rallison [13] used an ensemble average approach and a generalized reciprocal theorem to derive the average stress in a dilute suspension of drops in a second-order fluid. In the limit of high viscosity ratio, his results conform to those derived for rigid particles by Koch and Subramanian [11]. Since any viscoelastic fluid should behave as a second-order fluid in the limit of low shear rates, the aforementioned results will serve as a means of validating the present calculations for $\mathrm{De} \ll 1$. In addition to the three-dimensional suspension results noted above, the stress in a dilute suspension of circular particles in a two-dimensional second-order fluid was determined by Patankar and Hu [10] to complement their finite De numerical simulation study. For a two-dimensional second-order fluid the particle-induced polymer stress takes a simple form involving only a term representing the difference in the rates of strain inside and outside of the particles, because the flow field in this case, as indicated by the Tanner-Pipkin theorem, is unaltered from that for a Newtonian fluid.

The consideration of the Oldroyd-B constitutive equation for the rheology of the suspending fluid has several advantages for the present study. A well established experimental formulation known as a Boger fluid, consisting of a dilute solution of high molecular weight polymers in a viscous Newtonian fluid, yields rheology consistent with the equation [20–22]. A kinetic theory based on a Hookean dumbbell model of the polymers yields the Oldroyd-B constitutive equation [23]. It is common in computational studies to modify the model to incorporate finite extensibility

of the dumbbells in order to avoid stress singularities that may arise when the polymers experience extended periods of extensional motion such as at stagnation points at the rear of a fixed obstacle in the flow. However, the local Newtonian flow at all points in the fluid surrounding a neutrally buoyant particle in simple shear flow is a weak flow with a greater or equal amount of rotation as extension. Thus, Hookean dumbbells do not yield stress singularities in the present application and we retain the simplicity of the original Oldroyd-B formulation. The polymer concentration in the Oldroyd-B model can be adjusted to yield fluids in which the polymeric stress is small compared with the Newtonian stress even though the Deborah number is high and the polymer relaxation time is large. This feature will allow us to perform a perturbation analysis for small polymeric stress that still characterizes the shear-rate dependence of the suspension rheology. Because the shear viscosity and normal stress coefficients of Oldroyd-B fluids are independent of shear rate, they allow one to study the effects of fluid viscoelasticity in the absence of shear thinning of the suspending fluid. This feature is particularly valuable in the present study because it means that any shear-rate dependence of the rheology obtained from our calculations will be the result of particle-polymer interactions rather than being a feature of the underlying rheology of the polymeric fluid. Scirocco *et al.* [1] and Dai *et al.* [2] have measured the rheology of particle suspensions in Boger fluids and weakly shear thinning fluids and found that both the shear viscosity and the first normal stress coefficient shear thickened.

A potential complicating factor in the application of the present theory is the possibility that particles may cluster in a polymeric fluid to such an extent that most particles are not isolated from one another even in a dilute suspension. Clustering of particles has been observed experimentally in a variety of polymeric fluids [24–27]. However, it may be noted that Scirocco *et al.* [1] did not observe clustering in their rheological study of particle suspensions in Boger fluids and did not observe an evolution of the rheological properties over time as one might expect due to an extended period of structure development. In a theoretical study, Phillips and Talini [28] showed that widely separated particles in the flow-vorticity plane migrate toward one another in a second-order fluid. It is not clear from this study, however, what trajectories might occur in other parts of the flow where the mean shear flow drives relative motion. Yoon *et al.* [29] computed the motion of particle pairs started near one another in an Oldroyd-B fluid and found trajectories in which particles continue to move into closer proximity. However, the experimental observations of Snijkers *et al.* [30] of particle pairs in a Boger fluid found predominantly interactions in which particle pairs pass one another at larger separations than would occur in a Newtonian fluid. The contrasting results of these studies may arise from the choice of trajectories observed and it is possible that the numerically observed trajectories are relatively rare in a flowing suspension. Based on the experimental observations of [1,30], we postulate that most particles in a dilute suspension in a Boger fluid may be well separated. However, a more complete study of this phenomenon is desirable. If clustering were observed, an approach such as that of Highgate and Whorlow [5], who attempted to measure the rheology of a suspension in a non-Newtonian fluid before any structure would have time to develop, could be valuable.

The present analysis will consider the polymeric fluid as a continuum and will neglect the Brownian motion of the particles and the translational diffusion of the polymers as well as any effects associated with a finite ratio of the particle radius a to the polymer radius of gyration R_g. We will also neglect any effects of potential interactions between the particles and polymers. When particles are suspended in a Newtonian fluid, Brownian motion affects only the stress resulting from particle interactions and the $O(\phi)$ Einstein contribution to the viscosity is applicable to both Brownian and non-Brownian suspensions. The particle-polymer stress at $O(\phi)$ can be weakly influenced by the effect that the Brownian motion of the particles has on the sampling of relative positions of the polymer and particle. However, a larger influence on this sampling will come from the translational diffusion of the polymer whenever $R_g/a < 1$ and this effect will become important when a Péclet number $\mathrm{Pe}_{\mathrm{pol}} = \dot{\gamma} a^2/D_{\mathrm{pol}}$ based on the particle radius and the diffusivity of the polymer D_{pol} becomes $O(1)$. If R_g/a becomes $O(1)$ then the polymer will also experience effects of the nonlinearity of the flow over its extent, confinement effects due to the particle surface, and hydrodynamic reflections of the polymer velocity disturbance with the surface of the particle. Such

noncontinuum effects have been studied for polymer solutions in microchannels and nanochannels. Although the experiments at low particle volume fraction in [1] use small 2.7-μm-diam particles, the high viscosity of the fluid yields values of the Péclet number based on the particle diffusivity in the range from 6×10^3 to 6×10^6 and values of $\mathrm{Pe}_{\mathrm{pol}}$ in the range from 4×10^2 to 4×10^5, indicating that the influence of translational diffusion of the particles and polymers is modest. In addition, the ratio $a/R_g = 32$ suggests that noncontinuum effects are likely to be secondary but not completely negligible.

An important challenge in treating the average stress in a dilute suspension in a non-Newtonian fluid is to formulate the particles' effect on the polymer stress in a manner that leads to a convergent integral for the influence of each particle. The second-order fluid constitutive equation contains terms that are quadratic functions of the velocity gradient such as $\mathbf{e}\cdot\mathbf{e}$, where $\mathbf{e} = \frac{1}{2}(\boldsymbol{\nabla}\mathbf{u} + \boldsymbol{\nabla}\mathbf{u}^T)$ is the rate of strain and the superscript T indicates the transpose. Since the force dipole exerted by a neutrally buoyant particle in a low-Reynolds-number shear flow creates a disturbance to the rate of strain that decays with radial separation from the particle r as $1/r^3$, the volume integral that arises from a volume average of the stress is not convergent. However, using the ensemble average approach of [11,13], we have

$$\langle \mathbf{e}\cdot\mathbf{e}\rangle = \langle\mathbf{e}\rangle\cdot\langle\mathbf{e}\rangle + \langle\mathbf{e}'\cdot\mathbf{e}'\rangle = \langle\mathbf{e}\rangle\cdot\langle\mathbf{e}\rangle + n\int d\mathbf{r}_1\langle\mathbf{e}'\rangle_1\cdot\langle\mathbf{e}'\rangle_1, \tag{3}$$

where $\mathbf{e}' = \mathbf{e} - \langle\mathbf{e}\rangle$ is the disturbance to the mean strain rate, n is the number of particles per unit volume, and $\langle\,\rangle_1$ indicates the conditional ensemble average with one particle position fixed at $\mathbf{r}_1$. In the ensemble average formulation, the final integral, indicating the particle contribution to the mean polymer stress, has an integrand that decays as $|\mathbf{r}-\mathbf{r}_1|^{-6}$ with separation from the particle center and the integral converges. An important insight in this development is that the ensemble average of the linearized deviation of the stress from that based on the bulk strain rate is zero, i.e., $\langle\mathbf{e}'\cdot\langle\mathbf{e}\rangle\rangle = 0$. In the present application to an Oldroyd-B fluid, the polymer stress is determined by solving a differential equation over a Lagrangian trajectory rather than being a function of the local velocity gradient. However, we will be able to make use again of the insight that the average of the linearized disturbance to the polymer stress is zero to formulate a convergent expression for the influence of a particle on the mean polymer stress.

A second challenge is to determine the influence of the polymer rheology and the associated modification of the fluid velocity and pressure profile around the particle on the particle stresslet. One approach to this challenge would be a computational solution to the non-Newtonian flow around the particle. However, a generalized reciprocal theorem provides a means to determine the regular perturbation to mean particle properties such as the stresslet due to small deviations from Newtonian rheology in terms of the Newtonian fluid velocity field. Nearly all previous applications of a generalized reciprocal theorem to non-Newtonian flows have invoked a small Deborah number as the source of the small non-Newtonian effect, although Lauga [31] has recently shown that small particle deformation can serve as the perturbation parameter when evaluating non-Newtonian effects on the velocity of a microswimmer. In the present study we consider the small concentration of the high molecular weight polymer c as the perturbation parameter controlling the small non-Newtonian stress. An advantage of this choice, like that of Lauga, is that it allows one to explore viscoelastic behavior over a range of Deborah numbers.

In the following sections we formulate and compute the ensemble average stress in a dilute suspension of spherical particles in an Oldroyd-B fluid with small polymer concentration. In Sec. II we formulate the ensemble average stress. Section III provides a derivation of the particle contribution to the mean polymer stress. In Sec. IV the particle stresslet is derived with the aid of a generalized reciprocal theorem for evaluating influence of the perturbation to the Newtonian stress. Section V outlines the procedure for computing the integrals that arise from the theoretical formulation. Section VI provides a presentation of the results for the shear stress and first and second normal stress differences in the suspension as a function of the Deborah number. Finally, in Sec. VII we outline the conclusions of the present study and possible directions for future research.

II. ENSEMBLE AVERAGE STRESS

We consider a viscous, incompressible suspension with negligible inertia, so the mass and momentum conservation equations, valid in both the fluid and particle phase, are

$$\nabla \cdot \mathbf{u} = 0, \tag{4}$$

$$\nabla \cdot \boldsymbol{\sigma} = 0, \tag{5}$$

where $\mathbf{u}$ is the velocity field and $\boldsymbol{\sigma}$ is the overall stress tensor. The mean velocity field is specified to be a simple shear flow

$$\langle \mathbf{u} \rangle = \mathbf{e}_1 r_2, \tag{6}$$

where the angular brackets indicate an ensemble average over the suspension configuration, i.e.,

$$\langle A \rangle = \int d\mathbf{r}_1 \cdots d\mathbf{r}_N P(\mathbf{r}_1, \ldots, \mathbf{r}_N) A, \tag{7}$$

with P the probability density function for the particle positions $\mathbf{r}_1, \ldots, \mathbf{r}_N$. Here and in the subsequent development, lengths are nondimensionalized by the particle radius a, velocities by $\dot{\gamma} a$, and stresses by $\mu^s \dot{\gamma}$, where $\dot{\gamma}$ is the shear rate and μ^s is the viscosity of the solvent. The stress is expressed as the sum of a Newtonian solvent stress and a polymer stress $\boldsymbol{\Pi}$, i.e.,

$$\boldsymbol{\sigma} = \boldsymbol{\tau} + \boldsymbol{\Pi} = -p\boldsymbol{\delta} + 2\mathbf{e} + \boldsymbol{\Pi}, \tag{8}$$

where $\boldsymbol{\tau} = -p\boldsymbol{\delta} + 2\mathbf{e}$ is the Newtonian solvent stress and $\boldsymbol{\delta}$ is the identity tensor.

The polymer stress is defined as

$$\boldsymbol{\Pi} = c \frac{\boldsymbol{\Lambda}}{\mathrm{De}}, \tag{9}$$

where c is the polymer concentration and $\boldsymbol{\Lambda}$ is the polymer configuration tensor, defined as $\langle \mathbf{qq} \rangle$, where $\mathbf{q}$ is end-to-end relative position vector for a linear elastic dumbbell model of the polymer normalized by the radius of gyration of the polymer. The polymers do not enter the particles and so $\boldsymbol{\Pi}$ is defined to be zero within the particles. The Oldroyd-B constitutive equation specifies the evolution of the configuration tensor along Lagrangian trajectories as

$$\frac{D\Lambda_{ij}}{Dt} = \Lambda_{kj} \frac{\partial u_i}{\partial r_k} + \Lambda_{ik} \frac{\partial u_j}{\partial r_k} - \frac{1}{\mathrm{De}} (\Lambda_{ij} - \delta_{ij}), \tag{10}$$

where D/Dt indicates the convected derivative [23].

The ensemble average of the stress in the suspension may be written as

$$\langle \boldsymbol{\sigma} \rangle = -\langle p \rangle \boldsymbol{\delta} + 2\langle \mathbf{e} \rangle + \frac{c\langle \boldsymbol{\Lambda} \rangle}{\mathrm{De}} + n\mathbf{S}, \tag{11}$$

where n is the number of particles per volume and

$$\mathbf{S} = \int_{|\mathbf{r}-\mathbf{r}_1| \leqslant 1} d\mathbf{r}_1 \langle \boldsymbol{\sigma}^E \rangle_1 (\mathbf{r}|\mathbf{r}_1) \tag{12}$$

is the particle stresslet [32]. Here $\boldsymbol{\sigma}^E$ is the extra stress within the particle, in addition to that given by the fluid constitutive equations (8) and (9),

$$\langle A \rangle_1 (\mathbf{r}|\mathbf{r}_1) = \int d\mathbf{r}_2 \cdots d\mathbf{r}_N P(\mathbf{r}_2, \ldots, \mathbf{r}_N|\mathbf{r}_1) A \tag{13}$$

is the conditional ensemble average with one particle position fixed at $\mathbf{r}_1$, and $P(\mathbf{r}_2, \ldots, \mathbf{r}_N|\mathbf{r}_1)$ is the conditional probability density function. Since the rate of strain and polymer stress are both zero within the particle, the deviatoric part of the extra stress is equal to the deviatoric total stress.

Using this observation together with an application of the divergence theorem and the momentum equation (5) within the particle, the deviatoric part of the stresslet can be expressed as [32]

$$\hat{\mathbf{S}} = \int_{|\mathbf{r}_1-\mathbf{r}|=1} dA \left\{ \frac{1}{2}[\mathbf{nn}\cdot\langle\boldsymbol{\sigma}\rangle_1(\mathbf{r}|\mathbf{r}_1) + \mathbf{n}\cdot\langle\boldsymbol{\sigma}\rangle_1(\mathbf{r}|\mathbf{r}_1)\mathbf{n}] - \frac{1}{3}\boldsymbol{\delta}\mathbf{n}\cdot\langle\boldsymbol{\sigma}\rangle_1(\mathbf{r}|\mathbf{r}_1)\cdot\mathbf{n} \right\}, \tag{14}$$

where the caret indicates the deviatoric part of a tensor. In a sufficiently dilute suspension of well separated particles, the conditional average solvent and polymer stresses can be approximated as those surrounding an isolated particle and in the forthcoming development we will omit the conditional average symbols.

We seek a regular perturbation solution for small polymer concentration c and so expand the stress, stresslet, pressure, velocity, and polymer configuration in c, i.e., $\boldsymbol{\sigma} = \boldsymbol{\sigma}^0 + c\boldsymbol{\sigma}^1 + O(c^2)$, $\boldsymbol{\tau} = \boldsymbol{\tau}^0 + c\boldsymbol{\tau}^1, \mathbf{S} = \mathbf{S}^0 + c\mathbf{S}^1, p = p^0 + cp^1, \mathbf{u} = \mathbf{u}^0 + c\mathbf{u}^1$, and $\boldsymbol{\Lambda} = \boldsymbol{\Lambda}^0 + O(c)$. The leading-order fluid velocity and pressure field satisfy the Newtonian equations of motion and the solution for flow around a force- and torque-free particle with the fluid velocity approaching the average simple shear flow at large separations is

$$u_i^0 = E_{ji}r_j + \Omega_{ji}r_j + \frac{5}{2}\left(\frac{1}{r^7} - \frac{1}{r^5}\right)E_{jk}r_jr_kr_i - \frac{1}{r^5}E_{ji}r_j \quad \text{for } r \geqslant 1, \tag{15}$$

$$u_i^0 = \Omega_{ji}r_j \quad \text{for } r < 1, \tag{16}$$

and

$$p^0 = -\frac{5}{r^5}E_{jk}r_jr_k \quad \text{for } r \geqslant 1, \tag{17}$$

where

$$\boldsymbol{\Omega} = \tfrac{1}{2}(\boldsymbol{\nabla}\langle\mathbf{u}\rangle - \boldsymbol{\nabla}\langle\mathbf{u}\rangle^T) \tag{18}$$

and

$$\mathbf{E} = \tfrac{1}{2}(\boldsymbol{\nabla}\langle\mathbf{u}\rangle + \boldsymbol{\nabla}\langle\mathbf{u}\rangle^T) \tag{19}$$

are the mean vorticity and strain tensors.

III. AVERAGE POLYMER STRESS

The average of the polymer stress consists of two contributions, one resulting from the ensemble averaged fluid velocity gradients and a second caused by the particle-induced fluid velocity disturbances. To determine the $O(c)$ polymer contributions to the stress $c\langle\boldsymbol{\Lambda}^0\rangle/\mathrm{De}$ it is sufficient to compute the leading-order polymer configuration that is induced by the Newtonian fluid velocity field. It is useful to express the fluid velocity and rate of strain as $\mathbf{u} = \langle\mathbf{u}\rangle + \mathbf{u}'$ and $\mathbf{e} = \langle\mathbf{e}\rangle + \mathbf{e}'$, where $\mathbf{u}'$ and $\mathbf{e}'$ are the particle-induced fluid velocity and strain rate disturbances.

To motivate the strategy required to evaluate the average polymer stress, we recall the comparable approach used in the study of a suspension in a second-order fluid [11]. The second-order fluid stress includes terms that are nonlinear functions of the local fluid velocity gradient such as $\mathbf{e}\cdot\mathbf{e}$. This stress contribution may be written as a sum of a term that involves the undisturbed strain rate, a term that is linear in the disturbance, and a nonlinear term, i.e., $\mathbf{e}\cdot\mathbf{e} = \langle\mathbf{e}\rangle\cdot\langle\mathbf{e}\rangle + 2\langle\mathbf{e}\rangle\cdot\mathbf{e}' + \mathbf{e}'\cdot\mathbf{e}'$. The ensemble average of the term that is linear in the disturbance is zero, so $\langle\mathbf{e}\cdot\mathbf{e}\rangle = \langle\mathbf{e}\rangle\cdot\langle\mathbf{e}\rangle + \langle\mathbf{e}'\cdot\mathbf{e}'\rangle$. This observation is important, because it avoids the need to evaluate the linear term by integrating over the volume surrounding a test particle, which would have led to a nonconvergent integral since $\mathbf{e}' \sim 1/r^3$.

The polymer stress in a Boger fluid is obtained by solving the Oldroyd-B constitutive partial differential equation over fluid trajectories rather than being a function of the local velocity gradients.

Nonetheless, we can still write the polymer configuration as a sum

$$\mathbf{\Lambda}^0 = \mathbf{\Lambda}^{0U} + \mathbf{\Lambda}^{0L} + \mathbf{\Lambda}^{0N} \tag{20}$$

of a term $\mathbf{\Lambda}^{0U}$ that is driven by the undisturbed fluid velocity, one $\mathbf{\Lambda}^{0L}$ that has a linear dependence on the particle-induced perturbation to the fluid velocity, and one $\mathbf{\Lambda}^{0N}$ whose dependence on $\mathbf{u}'$ is nonlinear.

The polymer configuration due to the undisturbed fluid velocity is independent of spatial position and satisfies an equation

$$\frac{1}{\mathrm{De}}\mathbf{\Lambda}^{0U} = \boldsymbol{\nabla}\langle\mathbf{u}\rangle^T \cdot \mathbf{\Lambda}^{0U} + \mathbf{\Lambda}^{0U} \cdot \boldsymbol{\nabla}\langle\mathbf{u}\rangle \tag{21}$$

obtained by replacing the fluid velocity gradients in (10) with their ensemble averages. This equation can be solved analytically, and the components of the polymer configuration in the averaged flow are $\Lambda_{11}^{0U} = 1 + 2\mathrm{De}^2$, $\Lambda_{12}^{0U} = \mathrm{De}$, $\Lambda_{22}^{0U} = \Lambda_{33}^{0U} = 1$, and $\Lambda_{13}^{0U} = \Lambda_{23}^{0U} = 0$.

An equation for the linear response of the polymer configuration to the fluid velocity can be obtained by substituting the expansion (20) for the polymer configuration and $\mathbf{u} = \langle\mathbf{u}\rangle + \mathbf{u}'$ for the fluid velocity into the constitutive equation (10), subtracting the equation for the bulk configuration (21), and retaining only terms that are linear in $(\mathbf{u}', \mathbf{\Lambda}_0^L)$ to yield

$$\langle\mathbf{u}\rangle \cdot \boldsymbol{\nabla}\mathbf{\Lambda}^{0L} - \boldsymbol{\nabla}\langle\mathbf{u}\rangle^T \cdot \mathbf{\Lambda}^{0L} - \mathbf{\Lambda}^{0L} \cdot \boldsymbol{\nabla}\langle\mathbf{u}\rangle + \frac{1}{\mathrm{De}}\mathbf{\Lambda}^{0L} = \boldsymbol{\nabla}\mathbf{u}'^T \cdot \mathbf{\Lambda}^{0U} + \mathbf{\Lambda}^{0U} \cdot \boldsymbol{\nabla}\mathbf{u}'. \tag{22}$$

Since the disturbance to the velocity gradient decays as $1/r^3$, the solution for $\mathbf{\Lambda}_0^L$ obtained from (22) will also decay as $1/r^3$ at large distances $r \gg \max(1,\mathrm{De})$ from the particle where the polymer will have lost memory of the strain rate experienced close to the particle and the first term on the left-hand side of (22) may be neglected. The ensemble average of the equation for the linear polymer stress perturbation (22) leads to

$$\langle\mathbf{u}\rangle \cdot \boldsymbol{\nabla}\langle\mathbf{\Lambda}^{0L}\rangle - \boldsymbol{\nabla}\langle\mathbf{u}\rangle^T \cdot \langle\mathbf{\Lambda}^{0L}\rangle - \langle\mathbf{\Lambda}^{0L}\rangle \cdot \boldsymbol{\nabla}\langle\mathbf{u}\rangle + \frac{1}{\mathrm{De}}\langle\mathbf{\Lambda}^{0L}\rangle = 0. \tag{23}$$

The solution to this equation that decays at large distances from the particle is $\langle\mathbf{\Lambda}^{0L}\rangle = 0$.

Thus, the ensemble average of the polymer configuration can be expressed as the bulk stress plus the average of the nonlinear disturbance

$$\langle\mathbf{\Lambda}^0\rangle = \langle\mathbf{\Lambda}^{0U}\rangle + \langle\mathbf{\Lambda}^{0N}\rangle = \mathbf{\Lambda}^{0U} + n\int d\mathbf{r}_1\langle\mathbf{\Lambda}^{0N}\rangle_1. \tag{24}$$

The volume integral of the nonlinear polymer stress disturbance is convergent because the polymer stress terms that decay as slowly as $1/r^3$ have been captured by $\mathbf{\Lambda}^{0L}$. The nonlinear polymer stress can be obtained by solving (10) for the full polymer stress and then subtracting $\mathbf{\Lambda}^{0U}$ and $\mathbf{\Lambda}^{0L}$. While the full polymer stress is obtained by integrating (10) over fluid particle paths, the linearized disturbance is obtained by integrating (22) over streamlines of the undisturbed flow. The latter streamlines pass through the interior of the particle, so, although $\mathbf{\Lambda}^0 = 0$ in the interior, $\mathbf{\Lambda}^{0L}$, $\mathbf{\Lambda}^{0U}$, and $\mathbf{\Lambda}^{0N}$ are all nonzero therein. It may be noted that $\mathbf{e}' = -\mathbf{E}$ inside the particle and this provides a driving term in equation for the linear polymer stress perturbation (22) within the particle.

IV. STRESSLET

The particle stresslet, which quantifies the extra stress transmitted through the particles, is given by (14). The leading-order stresslet arising from the Newtonian solvent stresses is

$$\begin{aligned}\hat{\mathbf{S}}^0 &= \int_{|\mathbf{r}_1-\mathbf{r}|=1} dA\left(\frac{1}{2}[\mathbf{nn}\cdot\boldsymbol{\tau}^0 + \mathbf{n}\cdot\boldsymbol{\tau}^0\mathbf{n}] - \frac{1}{3}\boldsymbol{\delta}\mathbf{n}\cdot\boldsymbol{\tau}^0\cdot\mathbf{n}\right)\\ &= \frac{20\pi}{3}\mathbf{E}.\end{aligned} \tag{25}$$

The first correction to the stresslet for small polymer concentration can be factored into two contributions $\hat{\mathbf{S}}^1 = \hat{\mathbf{S}}^{1A} + \hat{\mathbf{S}}^{1B}$, where

$$\hat{\mathbf{S}}^{1A} = \frac{1}{\mathrm{De}} \int_{|\mathbf{r}_1 - \mathbf{r}|=1} dA \left(\frac{1}{2}[\mathbf{nn} \cdot \boldsymbol{\Pi}^0 + \mathbf{n} \cdot \boldsymbol{\Pi}^0 \mathbf{n}] - \frac{1}{3} \boldsymbol{\delta} \mathbf{n} \cdot \boldsymbol{\Pi}^0 \cdot \mathbf{n} \right) \tag{26}$$

results from the polymer stress acting at the particle surface and

$$\hat{\mathbf{S}}^{1B} = \int_{|\mathbf{r}_1 - \mathbf{r}|=1} dA \left(\frac{1}{2}[\mathbf{nn} \cdot \boldsymbol{\tau}^1 + \mathbf{n} \cdot \boldsymbol{\tau}^1 \mathbf{n}] - \frac{1}{3} \boldsymbol{\delta} \mathbf{n} \cdot \boldsymbol{\tau}^1 \cdot \mathbf{n} \right) \tag{27}$$

results from the first perturbations of the solvent stress due to polymer-induced changes in the fluid velocity and pressure fields. While $\hat{\mathbf{S}}^{1A}$ can be evaluated directly from the polymer configuration in the leading-order Newtonian velocity field, $\hat{\mathbf{S}}^{1B}$ would, in the form written in (27), require a numerical calculation of the fluid velocity in a non-Newtonian fluid. To avoid such a computational study and derive $\hat{\mathbf{S}}^{1B}$ directly from the Newtonian fluid velocity solution and the polymer configuration in this field, we make use of a generalized reciprocal theorem.

The first-order perturbation of the fluid velocity due to the polymer stress satisfies the equations

$$\boldsymbol{\nabla} \cdot \boldsymbol{\tau}^1 = -\frac{1}{\mathrm{De}} \boldsymbol{\nabla} \cdot \boldsymbol{\Lambda}_0, \tag{28}$$

$$\boldsymbol{\nabla} \cdot \mathbf{u}^1 = 0, \tag{29}$$

$$\boldsymbol{\tau}^1 = -p^1 \boldsymbol{\delta} + 2\mathbf{e}^1, \tag{30}$$

$$\mathbf{u}^1 = 0 \quad \text{at } r = 1, \tag{31}$$

$$\mathbf{u}^1 \to 0 \quad \text{as } r \to \infty. \tag{32}$$

The fluid velocity perturbation is driven by the divergence of the stress induced by the polymer deformation resulting from the $O(1)$ fluid velocity field. The velocity perturbation is zero on the particle and at large separations from the particle, because the $O(1)$ fluid velocity already satisfies the no-slip and imposed-shear-field boundary conditions.

The comparison field in the reciprocal theorem derivation must be chosen to yield a surface integral providing the property whose computation is desired. In this case, the particle stresslet is to be calculated and this suggests considering a comparison, Newtonian, fluid velocity field $\mathbf{v}$ that undergoes an extensional deformation on the particle surface and decays far from the particle, i.e.,

$$\boldsymbol{\nabla} \cdot \boldsymbol{\Sigma} = 0, \tag{33}$$

$$\Sigma_{ijkl} = -\delta_{ij} q_{kl} + \frac{\partial}{\partial r_i} v_{jkl} + \frac{\partial}{\partial r_j} v_{ikl}, \tag{34}$$

$$\boldsymbol{\nabla} \cdot \mathbf{v} = 0, \tag{35}$$

$$\mathbf{v} = \mathbf{B} \cdot \mathbf{r} \quad \text{at } r = 1, \tag{36}$$

$$B_{ijkl} = \tfrac{1}{2}\left(\delta_{ki}\delta_{lj} + \delta_{li}\delta_{kj} - \tfrac{2}{3}\delta_{kl}\delta_{ij}\right), \tag{37}$$

$$\mathbf{v} \to 0 \quad \text{as } r \to \infty. \tag{38}$$

The solution of the Stokes flow problem for the comparison velocity field is

$$v_{jkl} = \left(\frac{5}{2r^5} - \frac{5}{2r^7} \right) r_j r_k r_l + \frac{1}{2r^5}(r_k \delta_{jl} + r_l \delta_{jk}) + \left(\frac{1}{2r^5} - \frac{5}{6r^3} \right) r_j \delta_{kl}. \tag{39}$$

The reciprocal theorem is derived by applying the divergence theorem to the integral

$$\int_{V_f} dV \frac{\partial}{\partial r_i}\left(\tau^1_{ij} v_{jkl} - \Sigma_{ijkl} u^1_j\right) \tag{40}$$

and using the equations of motion and boundary conditions (28)–(38), to obtain

$$\int_{r=R_\infty} dA\, n_i \left(\tau^1_{ij} v_{jkl} - \Sigma_{ijkl} u^1_j\right) - \int_{r=1} dA\, n_i \tau^1_{ij} B_{jklm} r_m = -\int_{V_f} dV \frac{1}{\mathrm{De}} \frac{\partial \Lambda^0_{ij}}{\partial r_i} v_{jkl}, \tag{41}$$

where n_i is the unit normal vector pointing out of the particle or the surface at R_∞. The first integral is negligible as $R_\infty \to \infty$ because $\mathbf{u}^1$ and $\mathbf{v}$ decay as $1/r^2$ and the stresses decay as $1/r^3$ as $r \to \infty$. The second integral is the ij component of the deviatoric stresslet. Thus, the generalized reciprocal theorem demonstrates that the stresslet due to the non-Newtonian perturbation to the fluid velocity and pressure can be written in the form

$$\hat{\mathbf{S}}^{1B} = \int_{V_f} dV \frac{1}{\mathrm{De}} (\boldsymbol{\nabla} \cdot \boldsymbol{\Lambda}^0) \cdot \mathbf{v}. \tag{42}$$

While the equation (42) for the stresslet that comes directly from the generalized reciprocal theorem can be used to compute $\hat{\mathbf{S}}^{1B}$, it is not the most convenient form for the method of computation that we will adopt in Sec. V, where we will obtain the contributions to the stress in terms of integrals along the trajectories of fluid particles. Equation (42) requires an evaluation of the divergence of the polymer stress, which would necessitate interpolating the field from the Lagrangian points onto a fixed Eulerian grid to compute the derivative. To avoid this step, we employ the divergence theorem to transform (42) into

$$\hat{\mathbf{S}}^{1B} = \frac{1}{\mathrm{De}}\left[-\int_{r=1} dA\, \mathbf{n} \cdot \boldsymbol{\Lambda}^0 \cdot \mathbf{v} + \int_{r=R_\infty} dA\, \mathbf{n} \cdot \boldsymbol{\Lambda}^0 \cdot \mathbf{v} - \int_{V_f} dV\, \boldsymbol{\Lambda}^0 : \boldsymbol{\nabla} \mathbf{v} \right]. \tag{43}$$

The second term in (43) approaches zero as $R_\infty \to \infty$ because the integrand decays as $1/r^3$. Thus, the stresslet can be related to the sum of an area integral over the particle surface and a volume integral over the fluid. Each of these integrals involve the polymer stress but not its derivatives.

To summarize the results of the theoretical derivation, the deviatoric part of the ensemble average stress in a dilute particle suspension in a dilute polymer solution can be written as a dual regular perturbation expansion in the polymer concentration c and particle volume fraction ϕ as

$$\langle \hat{\boldsymbol{\sigma}} \rangle = \mathbf{T}^{00} + c\mathbf{T}^{10} + \phi \mathbf{T}^{01} + c\phi \mathbf{T}^{11}, \tag{44}$$

where

$$\mathbf{T}^{00} = 2\mathbf{E} \tag{45}$$

is the solvent viscous stress and

$$\mathbf{T}^{10} = \frac{1}{\mathrm{De}} \hat{\boldsymbol{\Lambda}}^{0U} \tag{46}$$

is the polymer stress based on the imposed shear flow. The bulk polymer stress components are $T^{10}_{12} = 1$ corresponding to the polymer contribution to the shear viscosity and $T^{10}_{11} - T^{10}_{22} = 2\,\mathrm{De}$ corresponding to the polymer contribution to the first normal stress difference. In addition, $T^{10}_{22} - T^{10}_{33} = 0$ as there is no second normal stress difference in a pure Oldroyd-B fluid and the other components are zero by symmetry. The Einstein contribution based on the solvent viscosity is reflected in

$$\mathbf{T}^{01} = 5\mathbf{E}. \tag{47}$$

Finally,

$$\mathbf{T}^{11} = \frac{3}{4\pi}(\hat{\mathbf{\Pi}}^{pp} + \hat{\mathbf{S}}^{1A} + \hat{\mathbf{S}}^{1B}) \tag{48}$$

is the first contribution to the stress caused by coupled effects of the particles and polymers whose computation is the goal of this paper. The first term on the right-hand side of (48) is the extra polymer stress induced by a particle, which is given by

$$\hat{\mathbf{\Pi}}^{pp} = \int_{V_f+V_p} dV \frac{1}{\mathrm{De}} \hat{\mathbf{\Lambda}}^{0N}, \tag{49}$$

where the integral is carried out over both the fluid V_f and particle V_p volumes. Here $\mathbf{\Lambda}^{0N}$ is the nonlinear perturbation to the polymer configuration caused by the particle which may be computed as described in Sec. III. The stresslet due to the polymer stress $\hat{\mathbf{S}}^{1A}$ will be computed using (26) and the stresslet due to the perturbation of the Newtonian stress by the polymers $\hat{\mathbf{S}}^{1B}$ is obtained from (43). It will also be convenient to define the $O(c\phi)$ contributions to the shear viscosity

$$\mu^{11} = T_{12}^{11}, \tag{50}$$

first normal stress coefficient

$$\psi_1^{11} = \frac{T_{11}^{11} - T_{22}^{11}}{\mathrm{De}}, \tag{51}$$

and second normal stress coefficient

$$\psi_2^{11} = \frac{T_{22}^{11} - T_{33}^{11}}{\mathrm{De}}. \tag{52}$$

We will also denote the contributions of the particle polymer stress and the stresslets $\hat{\mathbf{S}}^{1A}$ and $\hat{\mathbf{S}}^{2B}$ to ψ_1^{11} by ψ_1^{p11}, ψ_1^{A11}, and ψ_1^{B11}, respectively, with similar definitions for the respective contributions to the shear viscosity and second normal stress coefficient.

V. COMPUTATIONAL METHOD

The evaluation of the $\hat{\mathbf{S}}^{1B}$ contribution to the stresslet and the particle-induced polymer stress $\hat{\mathbf{\Pi}}_{pp}$ involves integrals of functions of the polymer stress over the volume of the fluid and the volume of both the particle and fluid, respectively. The fluid volume is unbounded. However, for computational purposes we consider a volume that is large compared with the sphere radius. The boundaries at large distances from the sphere are chosen to be at $r_3 = \pm r_{3\,\max}$, $r_2 = \pm r_{2\,\max}$, and $r_1 = r_{1\,\min}$ and $r_1 = r_{1\,\max}$, where $r_{2\,\max} = r_{3\,\max} = 40$, $r_{1\,\min} = -40$, and $r_{1\,\max} = 200$. The domain is chosen to be longer in the streamwise direction than in the gradient and vorticity directions because polymers that are deformed by interaction with the sphere can translate long distances in the r_1 direction before relaxing and this distance grows in proportion to De. These considerations cause us to limit our computations to $\mathrm{De} \leqslant 5$.

Since the polymer stress is computed by integrating (10) with the velocity field (15) along fluid trajectories, it would be most convenient if the volume integrals could also make use of fluid trajectories. It is intuitive to think that the integral of a quantity over the fluid volume in an incompressible flow would be equal to an area integral through an inlet or outlet to the volume of the volumetric flux times the time integral of the quantity over the fluid particle trajectories. A mathematical demonstration of this result can be obtained in the following manner.

The volume surrounding the particle in the Newtonian Stokes flow (15) can be subdivided into a region V_{open} consisting of streamlines extending infinitely far upstream and downstream of the particle in the r_1 direction and a region V_{closed} of closed streamlines circling around the particle. In the calculation of $\hat{\mathbf{\Pi}}_{pp}$, the interior of the particle is included within V_{closed}. Now consider a quantity

Q, such as a component of the nonlinear polymer stress $\frac{1}{\mathrm{De}}\hat{\mathbf{\Lambda}}^{0N}$, whose volume integral we wish to compute. Let P be the integral along a Lagrangian path of Q so that

$$P = \int_{t_0}^{t_1} Q\, dt', \tag{53}$$

where t_0 is the time at which the streamline enters V_{open} and t_1 is the time at which it reaches the point $\mathbf{r}$ of interest within the domain. Here Q is the convected derivative of P, which for an incompressible fluid at steady state is

$$Q = \frac{DP}{Dt} = \boldsymbol{\nabla}\cdot(\mathbf{u}P). \tag{54}$$

Performing a volume integral of (54) and applying the divergence theorem yields

$$\int_{V_{\mathrm{open}}} Q\, dV = \int_{A_{\mathrm{open}}} dA\, \mathbf{n}\cdot(\mathbf{u}P) = \int_{A_{\mathrm{exit}}} dA\left[\mathbf{n}\cdot\mathbf{u}\int_{t_0}^{t_1} Q\, dt'\right], \tag{55}$$

where A_{open} is the bounding area of the volume V_{open}, A_{exit} is the area $r_1 = r_{1\,\max}$ where streamlines exit the domain, and $\mathbf{n}$ is the outward unit normal to these surfaces. Here t_0 and t_1 are the times at which the streamlines enter and exit V_{open}. In the final equality we have used (53) and the facts that $P = 0$ at the inlet and that there is no flux across streamlines at the boundary between V_{open} and V_{closed}. To develop the comparable relationship for V_{closed}, we consider this volume to be bounded by surfaces A_{entrance} at $r_2 = \epsilon$ and $r_1 < 0$ and A_{exit} at $r_2 = -\epsilon$ and $r_1 < 0$ that lie just above and below the flow-vorticity plane and cut the closed streamlines. Defining $P = 0$ at $r_2 = \epsilon$ leads to a result equivalent to (55) for V_{closed}.

In a similar manner, the area integrals over the particle surface in the equations (26) and (43) for the stresslet $\hat{\mathbf{S}}^{1A}$ and $\hat{\mathbf{S}}^{1B}$ can be converted into integrals over the intersection of the spherical surface with the flow-vorticity plane of time integrals over the path of a polymer adjacent to the surface. The differential time along the polymer path is $dt = d\phi/u_\phi$ and the differential flux into the domain is $u_\phi \sin\theta\, d\theta$, where $u_\phi = \omega\sin\theta$ and ω is the angular velocity of the particle. Here θ is the azimuthal angle of a spherical coordinate system measured relative to the 3-axis and ϕ is the meridional angle in the 12-plane measured relative to the 1-axis. Thus, for example, the area integral in (43) can be computed using

$$\frac{1}{\mathrm{De}}\int_{r=1} dA\, \mathbf{n}\cdot\mathbf{\Lambda}^0\cdot\mathbf{v} = \frac{1}{\mathrm{De}}\int_0^{\pi/2}\sin\theta\, d\theta\int_0^{2\pi} d\phi\, \mathbf{n}\cdot\mathbf{\Lambda}^0\cdot\mathbf{v}. \tag{56}$$

The area integrals over A_{exit} are performed using Gaussian quadrature and the time integrals over the polymer trajectories using a fourth-order Runge-Kutta method. In the region of closed streamlines, the constitutive equation (10) is integrated over the closed loops repeatedly until the stress changes by less than 0.1% in one cycle before the particle-polymer stress and stresslet are computed. We determine the linearized stress $\mathbf{\Lambda}^{1L}$ on a fixed Eulerian grid by integrating (22) over the streamlines of the undisturbed flow and interpolate to obtain $\mathbf{\Lambda}^{1L}$ on the streamlines of the full velocity field when computing the volume integral of $\mathbf{\Lambda}^{1N}$. While $\mathbf{\Lambda}^1$ is a smooth function of position at all De, the linearized polymer stress has a boundary layer of thickness De inside and outside of the particle surface when $\mathrm{De} \ll 1$. This boundary layer arises because the strain rate undergoes a step change at the particle surface. To improve the accuracy of the computation at small Deborah numbers, we add and subtract an analytical description of the stress due to this step change of strain rate so that the remaining stress that must be computed numerically is smooth. Based on the symmetry of the problem, we can compute the integrals over the open streamline domain for $r_2 > 0$ and $r_3 > 0$ and multiply the resulting integral by 4. The integrals over the closed streamline domain can be computed for $r_3 > 0$ with the result multiplied by 2.

An indication of the accuracy of the computations can be obtained by comparing our results for the various stress contributions at small Deborah numbers to the analytical predictions [11] of

TABLE I. Comparison of the stress contributions at small Deborah number obtained from our computations for an Oldroyd-B fluid and the analytical predictions [11] for a second-order fluid.

Quantity	Computation	Analysis
μ^{11}	2.52	2.5
μ^{11p}	0.02	0
μ^{11A}	1.50	1.5
μ^{11B}	1.00	1
ψ_1^{11}	5.08	5
ψ_1^{11p}	0.10	0
ψ_1^{11A}	3.00	3
ψ_1^{11B}	1.98	2
ψ_2^{11}	0.09	0.18
ψ_2^{11p}	1.68	1.79
ψ_2^{11A}	−1.49	−1.5
ψ_2^{11B}	−0.10	−0.11

the normal stress coefficients for a second-order fluid and the shear stresslet due to the polymer contribution to the Newtonian viscosity. This comparison is shown in Table I. The analytical results make use of the first and second normal stress coefficients of the Oldroyd-B suspending fluid, which, in dimensionless form, are $\psi_1^{10} = 2$ and $\psi_2^{10} = 0$. It may be seen that in general the computations provide an excellent reflection of not only the overall viscosity and normal stress coefficients but also the respective contributions of the particle-induced polymer stress (superscript p), the direct polymer contribution to the stresslet (superscript A), and the stresslet due to the flow modification (superscript B). Among the various contributions to the stress, a maximum deviation of about 5% occurs for the particle-polymer contribution to the second normal stress difference. This error may be attributed primarily to the limited size of the computational domain.

VI. RESULTS AND DISCUSSION

The $O(c\phi)$ contribution to the shear viscosity μ^{11} is plotted as a function of the Deborah number in Fig. 1 along with its contribution μ^{11p} from the particle-induced polymer stress and the particle stresslet. The particle stresslet contributions to μ^{11} are also plotted separately in Fig. 2. The low-Deborah-number limits of the results are compared with theory in Table I. The stresslet at low Deborah number is in good agreement with that expected based on the Einstein viscosity contribution, $(5/2)\phi c\mu^s$ in unscaled form, resulting from the polymer contribution $c\mu^s$ to the zero-shear-rate viscosity. Within this stresslet a contribution $3/2$ comes from the shear stress and is captured by μ^{11A}, the direct influence of the deviatoric polymer stress on the stresslet, while the pressure contribution 1 is found in μ^{11B} as the stresslet due to the modified solvent stress. The computed μ^{11p} of 0.02 is close to the value 0 obtained theoretically. A retarded motion expansion [23] for a non-Newtonian fluid indicates that the shear viscosity should remain unaltered at $O(\mathrm{De})$, corresponding to a second-order fluid, and the approximate zero slope of the curves for μ^{11} and its components at $\mathrm{De} = 0$ is consistent with this prediction.

The most striking aspect of the results in Fig. 1 is a substantial shear thickening of the particle-polymer shear viscosity at Deborah numbers larger than about 1. The shear viscosity grows approximately linearly with the Deborah number for $\mathrm{De} = 3$–5 and reaches a value more than 5 times larger than its zero-shear-rate asymptote at $\mathrm{De} = 5$. The shear thickening results from the particle-induced polymer stress μ^{11p}, while the stresslet contributions shear thin. The primary reason for the linear increase of the particle-induced polymer shear stress with De is that polymers,

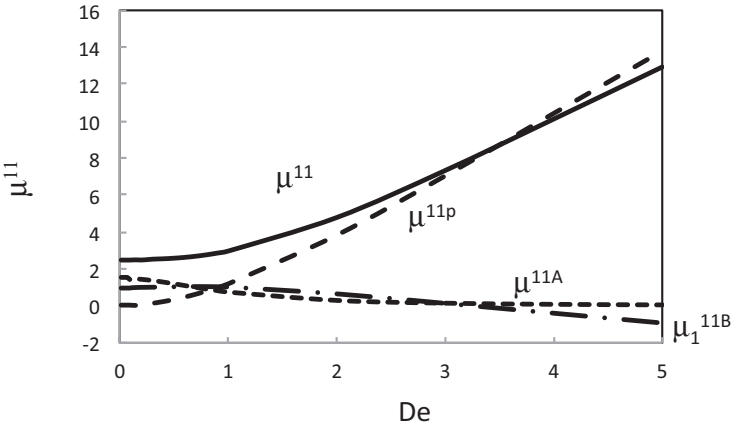

FIG. 1. Contributions of particle-polymer interactions to the shear viscosity plotted as functions of the Deborah number: μ^{11} (solid line) is the overall $O(c\phi)$ contribution, μ^{11p} (long-dashed line) is the particle-induced polymer stress, and μ^{11A} (short-dashed line) and μ^{11B} (dash-dotted line) are the stresslet due to the polymer stress and the polymer-induced modification of the Newtonian stress, respectively.

which come within a separation of a few particle radii, are stretched by the particle's fluid velocity disturbance and are convected downstream of the particle in a wake of $O(\mathrm{De})$ length before they relax. Thus, the volume of fluid containing a nonlinear polymer stress grows in proportion to De.

Scirocco *et al.* [1] have observed shear thickening of the viscosity of suspensions of 2.7-μm-diam polystyrene spheres in a Boger fluid (which they call BF1) and a slightly shear thinning (SST) fluid. These fluids consist of solutions of the same high molecular weight polyisobutylene in the same Newtonian polybutene solvent with the concentration of the high molecular weight polymer being 5 times larger in the SST fluid. The lowest volume fraction studied was $\phi = 0.068$. Shear thickening of the viscosity was also observed in experiments of Dai *et al.* [2] using 42-μm-diam poly(methyl methacrylate) spheres in a solution of polyacrylamine in a mixture of corn syrup, glycerin, and water that was designed to approximate a Boger fluid but exhibited slight shear thinning similar to the SST fluid of Scirocco *et al.* The lowest volume fraction in the study of Dai *et al.* was $\phi = 0.05$.

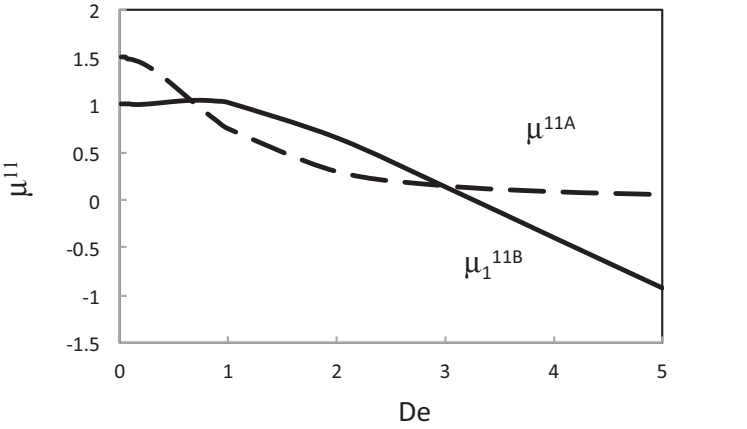

FIG. 2. Stresslet contributions to the shear viscosity plotted as a function of the Deborah number. The dashed line μ^{11A} and solid line μ^{11B} are the stresslet due to the polymer stress and the polymer-induced modification of the Newtonian stress, respectively.

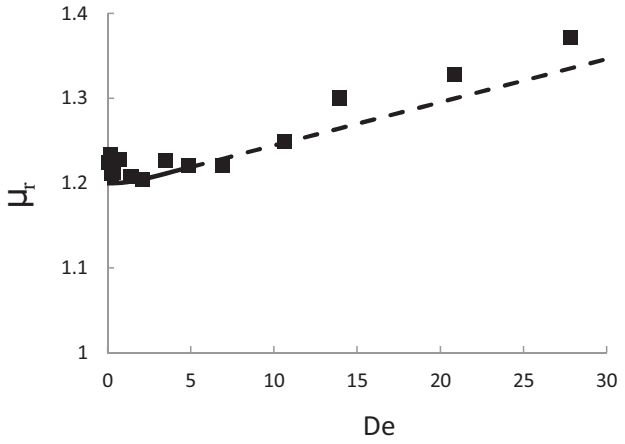

FIG. 3. Predictions for the relative viscosity of a polymer-particle suspension compared with the experimental measurements of Scirocco *et al.* [1] for a suspension with $\phi = 0.068$ in Boger fluid BF1. The squares are the experimental measurements. The solid line is the prediction of the present theory and the dashed line is an extrapolation of these predictions assuming that the linear growth of μ^{11} with De observed for De = 3–5 continues at higher Deborah numbers.

Using the measured zero-shear-rate viscosity μ^0 and solvent viscosity μ^s of the SST and Dai *et al.* fluids, we estimate the polymer concentration as $c = \mu^p/\mu^s = 0.13$ and 0.42, respectively. Here $\mu^p = \mu^0 - \mu^s$ is the polymer contribution to the zero-shear-rate viscosity. Since the difference between μ^0 and μ^s lies within the measurement uncertainty for BF1, we use the measurement of c for the SST fluid and assume that the ratio of c for SST and BF1 is the same (5) as the ratio of the parts per million of polyisobutylene in these two fluids. This yields a polymer concentration $c = 0.027$ and relaxation time $\lambda = \psi_1^{10}/2\mu^p = 6.9$ s for the BF1 fluid. Although suspensions based on all three fluids show shear thickening above a critical Deborah number in qualitative agreement with the theoretical predictions, we believe that the moderate values of c and the shear thinning behavior, that deviates from an Oldroyd-B fluid and may also induce particle clustering, make the SST and Dai *et al.* suspensions inappropriate for a comparison of the degree of shear thickening. The degree of shear thickening due to particle-polymer interactions is proportional to $c\phi$ where the theory requires $c \ll 1$ and $\phi \ll 1$. This clearly leads to a challenge in comparing theory with experiments and indeed the small value $c\phi = 1.8\times10^{-3}$ for the $\phi = 0.068$ BF1 suspension leads to measurable shear thickening only for De > 10. To make a comparison with the theoretical prediction, we assume that the linear increase of μ^{11} with De observed in the range De = 3–5 continues at higher Deborah numbers so that $\mu^{11} = 12.93 + 2.82(\text{De} - 5)$ for De = 5–30. Owing to the moderate concentration of the particles, it is important to incorporate the effect of pair interactions on the zero-shear-rate viscosity of the suspension in the comparison. To do so we use Batchelor's [32] result for the effects of pair interactions in a sheared suspension and estimate the relative viscosity of the suspension as $\mu^r = \mu/\mu^0(\phi = 0) = 1 + 2.5\phi + 6\phi^2 + c\phi(\mu^{11} - 2.5)$, where the subtraction of 2.5 from the $O(c\phi)$ term accounts for the fact that this factor is already included in the zero-shear-rate viscosity of the suspension. The resulting comparison of the relative viscosity predicted by the present theory with the measurements of Scirocco *et al.* [1] is shown in Fig. 3. Both the extrapolated theory and the experiments show that the particle contribution to the viscosity shear thickens by about a factor of 2 up to a Deborah number of 30.

Both stresslet contributions to the shear viscosity exhibit shear thinning. The stresslet due to the direct effect of the deviatoric polymer stress μ^{11A} results from the behavior of polymers circling the particles on closed streamlines directly adjacent to the particle surface. In a reference frame rotating with the particle, a polymer at the particle surface sees the Newtonian fluid velocity field as a local

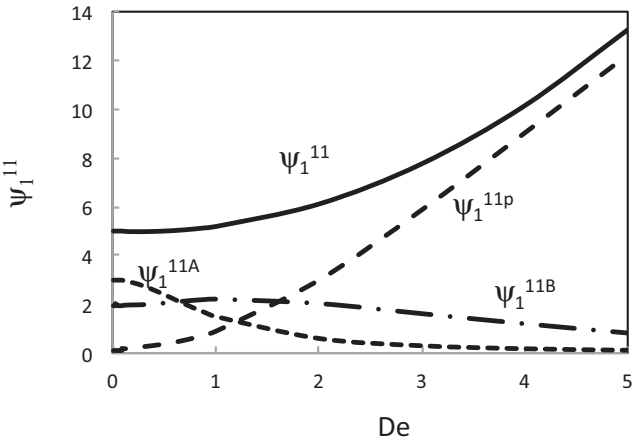

FIG. 4. Contributions of particle-polymer interactions to the first normal stress coefficient plotted as a function of the Deborah number: ψ_1^{11} (solid line) is the overall $O(c\phi)$ contribution, ψ_1^{11p} (long-dashed line) is the particle-induced polymer stress, and ψ_1^{11A} (short-dashed line) and ψ_1^{11B} (dash-dotted line) are the stresslet due to the polymer stress and the polymer-induced modification of the Newtonian stress, respectively.

simple shear flow with a time periodic shear rate $\frac{\partial u_\phi}{\partial r} = \frac{3}{2}\sin\theta\cos(2\phi)$ and $\frac{\partial u_\theta}{\partial r} = \frac{5}{4}\sin(2\theta)\sin(2\phi)$, where $\phi = \omega t$. At high Deborah numbers, the polymer relaxation time eventually becomes larger than the period of rotation and the polymer stretch will decay as the polymer responds to a time-averaged zero shear rate. In addition, the polymer stress has a factor of $\frac{1}{\mathrm{De}}$ because it is an elastic rather than viscous stress. As a result, we may expect μ^{11A} to be proportional to De^{-2} at high Deborah numbers. Although the Deborah numbers in the computation are not high enough to strictly access this limit, the results are qualitatively consistent with this expectation.

The stresslet caused by the alteration of the Newtonian solvent stress μ^{11B} shear thins and eventually becomes negative at Deborah numbers larger than about 3.3. Since we used the generalized reciprocal theorem to evaluate this contribution without the need to derive the perturbed fluid velocity resulting from polymeric stresses, we cannot directly assess the mechanism for the shear thinning and the eventual negative stresslet from the present study. However, the Snijkers *et al.* [33] results for viscoelastic shear flow around a neutrally buoyant particle (Fig. 10 of [33]) indicate that the maximum shear rate in the 12-plane is shifted downstream of the gradient direction and the maximum normal stress is shifted downstream of the extensional axis of the imposed flow with increasing De. Both these changes would reduce the stresslet due to the Newtonian solvent.

The $O(c\phi)$ first normal stress coefficient ψ_1^{11} due to particle-polymer interactions is plotted as a function of the Deborah number in Fig. 4 along with the particle-induced polymer stress and particle stresslet contributions. The stresslet contributions are plotted separately in Fig. 5. As shown in Table I, the computed low-Deborah-number limit of the stresslet, 4.98, is very close to the theoretical prediction, 5, for a second-order fluid. The ratio of the first normal stresslet contribution to the fluid first normal stress coefficient, 2.5, is equal to the ratio of the shear stresslet to the fluid viscosity and it has been noted [11] that this simple result arises because the first normal stresslet is caused by a solid-body rotation of the fluid pressure and polymer stress field that produce the shear stresslet. The computed particle-induced stress contribution ψ_1^{11p} is 0.1 at small Deborah number, while the theoretical prediction is 0.

The first normal stress coefficient due to particle-polymer interactions, like the viscosity, shear thickens. It grows approximately quadratically with Deborah number at Deborah numbers larger than about 1. The shear thickening again results from the growing particle-induced polymer stress ψ_1^{11p}, whereas the first normal stresslet shear thins. Since $\psi_1^{11} = \frac{T_{11}^{11} - T_{22}^{11}}{\mathrm{De}}$, its quadratic growth with

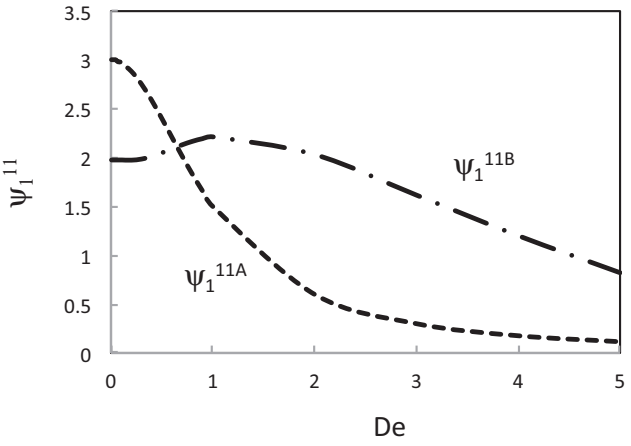

FIG. 5. Stresslet contributions to the first normal stress coefficient plotted as a function of the Deborah number. The dashed line ψ_1^{11A} and solid line ψ_1^{11B} are the stresslet due to the polymer stress and the polymer-induced modification of the Newtonian stress, respectively.

De implies that the normal stress difference grows as De^3. The plot in Fig. 6 of the polymer stress on an open streamline that passes through the wake downstream of the particle indicates that the 11 polymer stress Λ_{11}^0/De grows quadratically in amplitude in the wake with increasing De and the wake length grows linearly with De. The combination of these effects results in the cubic growth of the normal stress difference. The alignment of the polymers with the streamlines in the wake makes particle-induced stress larger than the particle-induced shear stress at large De.

Scirocco *et al.* [1] observed shear thickening of the first normal stress coefficient of particle suspensions in BF1 and SST fluids. Similarly, Dai *et al.* [2] observed shear thickening of the first normal stress coefficient in suspensions in their polyacrylamide–corn syrup viscoelastic fluid. A comparison of predictions for the relative first normal stress difference ψ_1/ψ_1^0, where ψ_1^0 is the zero-shear-rate first normal stress coefficient of the suspending fluid, with the BF1 fluid $\phi = 0.068$ experiments of Scirocco *et al.* is given in Fig. 7. The theoretical comparison makes use of the

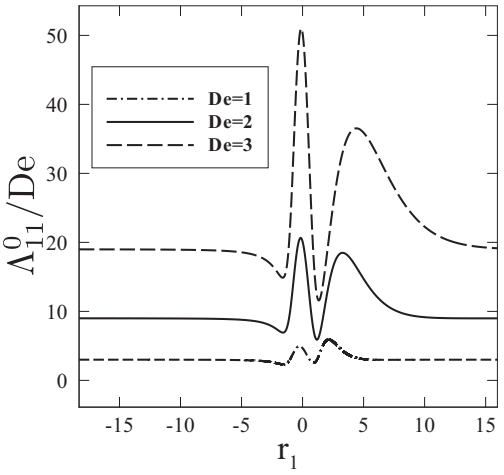

FIG. 6. The 11-component of the polymer stress along an open streamline starting at $r_1 = -200$, $r_2 = 0.5$, and $r_3 = 0$ plotted for De = 1, 2, and 3.

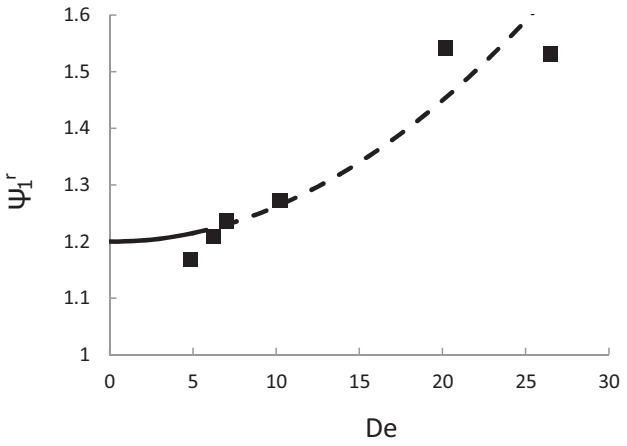

FIG. 7. Predictions for the relative first normal stress coefficient of a polymer-particle suspension compared with the experimental measurements of Scirocco *et al.* [1] for a suspension with $\phi = 0.068$ in Boger fluid BF1. The squares are the experimental measurements. The solid line is the prediction of the present theory and the dashed line is an extrapolation of these predictions assuming that the quadratic growth of ψ_1^{11} with De observed for De = 3–5 continues at higher Deborah numbers.

quadratic dependence of ψ_1^{11} on De in the De = 3–5 range to extrapolate the results for De = 5–30 as $\psi_1^{11} = 13.26 + 0.346(\mathrm{De}^2 - 25)$. The relative first normal stress coefficient of the suspension is then $\psi_1^r = 1 + 5\phi + c\phi(\psi_1^{11} - 5)$. The extrapolated theory and experiment both exhibit shear thickening of the first normal stress coefficient by about a factor of 4 up to De = 30.

The stresslet contributions to the first normal stress coefficient in Fig. 5 shear thin in a qualitatively similar manner to the stresslet contributions to the shear viscosity in Fig. 2, although ψ_1^{11B}, unlike μ^{11B}, remains positive over the range of Deborah numbers we explore. The direct contribution of the deviatoric polymer stress on closed streamlines circling the particle ψ_1^{11A} decays rapidly to zero as the polymer relaxation time becomes large enough so that the polymer responds to the zero average shear rate over a period of the particle rotation. One reason for the shear thinning of ψ_1^{11B} is the decrease in the pressure in the wake at the downstream portion of the sphere as seen in numerical simulations of the non-Newtonian flow in Fig. 9 of [33].

The results for the second normal stress coefficient and its various components as functions of Deborah number are plotted in Fig. 8 and the comparison of these results with theoretical predictions for a second-order fluid at low Deborah number are listed in Table I. Figure 9 gives a clearer view of the results for ψ_2^{11} and ψ_2^{11A} whose magnitudes are smaller than ψ_2^{11B} and ψ_2^{11p}. The results for the second normal stress coefficient are the most subtle and difficult to compute of the three fluid properties because the overall second normal stress coefficient is small and results from a large positive contribution from the polymer-induced stress and a large negative contribution from the stresslet. At low Deborah numbers, the second-order fluid calculation [11] yields a large positive contribution of the particle-induced polymer stress $\psi_2^{11p} = 1.78$ and the computation yields $\psi_2^{11p} = 1.68$. The theoretical and computational stresslet contributions are -1.61 and -1.59, respectively, and the overall second normal stress coefficients from theory and computations are $\psi_2^{11} = 0.18$ and 0.09.

The particle-induced polymer second normal stress coefficient ψ_2^{11p} shear thickens but its variation with De is much more modest than that of μ^{11p} and ψ_1^{11p}. This results from the fact that the particle's disturbance velocity modulates the 22 and 33 polymer stresses only in an $O(1)$ region around the particle. In the wake, the polymers that have been stretched by the particle fluid velocity disturbance are rotated toward the flow direction and only the 11 and 12 stresses remain.

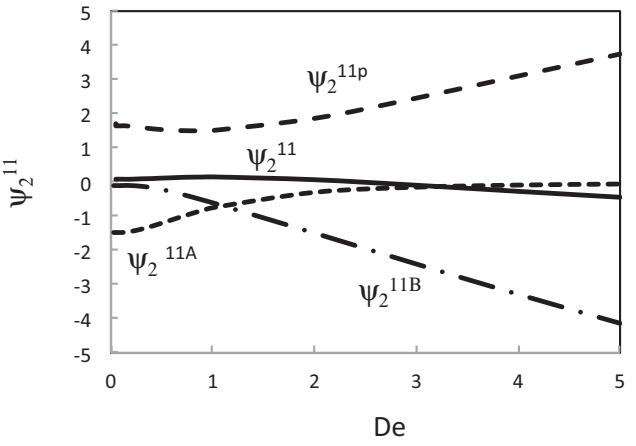

FIG. 8. Contributions of particle-polymer interactions to the second normal stress coefficient plotted as a function of the Deborah number: ψ_2^{11} (solid line) is the overall $O(c\phi)$ contribution, ψ_2^{11p} (long-dashed line) is the particle-induced polymer stress, and ψ_2^{11A} (short-dashed line) and ψ_2^{11B} (dash-dotted line) are the stresslet due to the polymer stress and the polymer-induced modification of the Newtonian stress, respectively.

The second normal stresslet contribution for a second-order fluid was determined to be negative [11]. The direct contribution of the polymers on closed streamlines adjacent to the particle ψ_2^{11A} decays to zero with increasing Deborah number as the polymers begin to experience the zero mean shear rate along a closed path. On the other hand, the influence of the polymer on the Newtonian stress results in an increasingly large negative contribution to the second normal stress coefficient with increasing shear rate. This is consistent with the comment of Snijkers *et al.* [33] that their viscoelastic flow simulations exhibited an increasing-high-pressure region near the 12-plane and a low-pressure region near the 3-axis with increasing De. The net effect of the positive but slowly varying particle-induced polymer stress contribution and the increasingly negative stresslet contribution is that the overall particle-polymer second normal stress coefficient ψ_2^{11} starts at a modest positive value at low Deborah numbers, grows slightly for De = 0–1, and then decays, becoming negative for De $>$ 2.3.

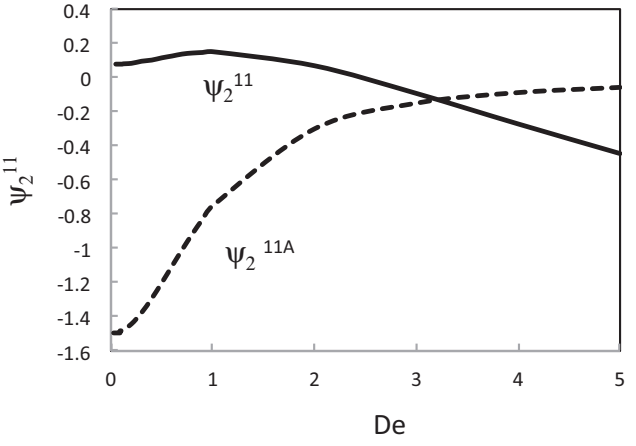

FIG. 9. Overall contribution of particle-polymer interactions to the second normal stress coefficient (solid line) plotted as a function of the Deborah number along with the stresslet due to the polymer stress ψ_2^{11A} (short-dashed line).

The shear-rate dependence of ψ_2^{11} has not been explored experimentally. However, Tanner *et al.* [3] measured the second normal stress coefficient in particle suspensions with volume fractions $\phi = 0.05$ and larger in a Boger fluid consisting of polyacrylamide in a corn syrup, glycerin, and water mixture. Contrary to the predictions of the low-Deborah-number theory, Tanner *et al.* [3] observed a negative contribution of the particles to the second normal stress coefficient. The present theory would predict such a contribution for $\mathrm{De} > 2.3$, but the measurements were conducted for De values from about 0.05 to 0.5.

As noted by Tanner *et al.* [3], their measurements would be consistent with a scenario in which the negative particle stresslet contribution to ψ_2^{11} is evident but the positive ψ_2^{11p} is attenuated as a result of interactions among the clouds of disturbed polymers surrounding neighboring particles. The results in Fig. 6 corroborate their intuition that a criterion of nonoverlapping polymer stress fields could be quite stringent. It can be seen that the wake length in Fig. 6 is about 4 De. Taking the volume of the wake as $4\times4\times4\max(1,\mathrm{De})$, the criterion for a dilute suspension with nonoverlapping polymer fields would be $n64\max(1,\mathrm{De}) \ll 1$ or $\phi \ll \frac{1}{16\max(1,\mathrm{De})}$. This would suggest that a value smaller than $\phi = 0.05$ is required to obtain a truly dilute suspension of particles with noninteracting polymer clouds at low Deborah numbers with an even more stringent criterion as the Deborah number grows. It need not be the case, however, that the interactions of polymer clouds would always reduce the particle-induced polymer stress. In a study of a semidilute fiber suspension in an Oldroyd-B fluid, Harlen and Koch [34] showed that rotation and stretching of polymers by successive fibers could greatly increase the shear viscosity. Since the wakes downstream of particles are populated primarily by polymers realigning with the streamlines, this coupled enhancement of the stress can be expected to contribute to a synergistic shear thickening of the shear viscosity and first normal stress coefficients. The effect of overlapping wakes on the polymer stress contribution to the second normal stress coefficient is more difficult to anticipate theoretically and appears from the experimental study of [3] to be an attenuation.

VII. CONCLUSION

We have derived the first effects of particle-polymer interactions on the shear-dependent rheology of dilute particle suspensions in dilute polymer solutions. The polymer stress was governed by the Oldroyd-B constitutive equation, which has the interesting feature of predicting no shear thinning of the viscosity and first normal stress coefficient of the suspending fluid. The shear-rate dependence of the ensemble average stress in the suspension resulted from the polymeric stress in the fluid, which was influenced by the velocity disturbances caused by the particles, and from particle stresslets, which were influenced by the direct effects of the polymer stress and the indirect effects due to polymer-induced fluid velocity and pressure modifications.

Two crucial features of the theoretical development were the derivation of an expression for the particle-induced polymer stress that is convergent when integrated in an unbounded fluid region surrounding a test particle and the use of a generalized reciprocal theorem to obtain the stresslet without the requirement of directly computing the flow modification caused by the polymers. The derivation of the average particle-induced polymer stress involved making the observation that a polymer stress that is linearized for weak fluid velocity disturbances has an ensemble average of zero. One can then express the total ensemble average polymer stress as a contribution due to the imposed shear flow with no particle influence and a term due to the nonlinear perturbation of the polymer stress by the particle velocity disturbance. The latter term is convergent when integrating in the region around a single particle. Our treatment of the stresslet uses the common strategy for weakly non-Newtonian suspension flows of applying a generalized reciprocal theorem to derive perturbed particle properties without a detailed perturbed velocity field calculation but uses a small polymer concentration in place of a small polymer relaxation time as the perturbation parameter.

It would be of interest to extend the present analysis to a wider range of rheological models and, perhaps more importantly, to more strongly non-Newtonian fluids. This could be accomplished by

combining the present ensemble average analysis with a full numerical solution of the fluid velocity and pressure and the polymer stress in the flow around a spherical particle in simple shear flow such as those in [33,35,36]. In such a study the numerical solution of the perturbed velocity and pressure would remove the need for a generalized reciprocal theorem. However, one would still need to follow the procedures outlined in Secs. III and V to subtract the linear perturbation to the polymer stress in order to obtain a convergent integral for the particle-induced polymer stress. A numerical challenge in such a study would be to have a large enough computational domain to capture the full extent of the region of disturbed polymers, including the wake whose length grows with De, while still providing adequate grid resolution near the particle and across the transverse dimensions of the wake.

The analysis could also be extended to unsteady flows such as the start up of steady shear flow or large-amplitude oscillatory shear flow. The ensemble average of the linearized polymer stress remains zero in the unsteady problem and the strategy for renormalization used in the present study could still be applied.

We derived the $O(c\phi)$ contributions to the shear viscosity and the first and second normal stress coefficients over a range of Deborah numbers from 0 to 5. The results were generally in good agreement with previous predictions [11,14] for the low-Deborah-number limit, although the near cancellation of contributions to the second normal stress coefficient ψ_2^{11} made the computation of the individual contributions of stresslet and polymer stress more accurate than the overall ψ_2^{11} at low De. The most striking results of the computation were strong shear thickening of the particle-polymer contributions to the shear viscosity and first normal stress coefficient for $\mathrm{De} > 1$. This theoretical prediction is in agreement with observations by Scirocco *et al.* [1] of shear thickening of both these properties in particle-filled Boger fluids. The theoretical calculation demonstrates that this shear thickening results from an increase of the particle-induced polymer stress as the wake of disturbed polymers downstream of the particles becomes increasingly long. The shear and first normal stress components of the stresslet of the particle shear thin. The particle-polymer contribution to the second normal stress coefficient, which has a very small positive value in the low-Deborah-number limit, decreases with increasing Deborah number and becomes negative at $\mathrm{De} = 2.3$. In contrast to the other two rheological properties, the shear-rate dependence of the second normal stress coefficient comes primarily from the increasingly negative stresslet. The particle-induced second normal polymer stress has a weaker shear-rate dependence than its shear and first normal stress counterparts because the second normal stress disturbance due to the particles is localized to the particle neighborhood and does not extend far into the wake.

A better understanding of the rheology of dilute and moderately concentrated particle suspensions in viscoelastic fluids could be obtained from more extensive experimental and multiparticle simulation studies in this regime. The most dilute particle suspensions that have been studied to date [1,3] have $\phi \approx 0.05$–0.07 and these studies do not vary ϕ within this dilute (or semidilute) regime. Studies that achieve lower ϕ would provide a better test of the noninteracting particle theory and studies that vary ϕ would resolve the question of whether particle-induced polymer cloud interactions are important at semidilute concentrations. It would also be of interest to measure the shear-rate dependence of the second normal stress coefficient. Birefringence measurements could provide direct access to the particle-induced polymer stress, so one could test the individual contributions to the rheological properties and not just their net values. Because the role of any possible particle clustering on suspension rheology is not yet well understood, it would be valuable to have experiments or multiparticle simulations that examine the pair probability for the same system in which a rheological characterization is performed. The experimental observation [1] that shear thickening of viscosity and the first normal stress coefficient, which is predicted here for dilute particle suspensions, continues to be observed at $\phi \approx 0.3$ suggests that even when the clouds of polymers disturbed by particles strongly overlap, the polymer stretching by the particles has a striking effect on rheology. Thus, one should not think of the stress in a filled polymer fluid as resulting from independent contributions of the particles and polymers but from their synergistic effects. The present study has clarified some aspects of those synergistic effects by providing a theoretical prediction for the limiting case of small particle and polymer concentrations.

ACKNOWLEDGMENT

This work was supported by NSF Grant No. CBET-1435013.

[1] R. Scirocco, J. Vermant, and J. Mewis, Shear thickening in filled Boger fluids, J. Rheol. **49**, 551 (2005).
[2] S. Dai, F. Qi, and R. I. Tanner, Viscometric functions of concentrated non-colloidal suspensions of spheres in a viscoelastic matrix, J. Rheol. **58**, 183 (2014).
[3] R. I. Tanner, S. Dai, F. Qi, and K. Housiadas, Viscometric functions of semi-dilute non-colloidal suspensions of spheres in a viscoelastic matrix, J. Non-Newton. Fluid Mech. **201**, 130 (2013).
[4] B. A. Haleem and P. R. Nott, Rheology of particle-loaded semi-dilute polymer solutions, J. Rheol. **53**, 383 (2009).
[5] D. J. Highgate and R. W. Whorlow, Rheological properties of suspensions of spheres in non-Newtonian media, Rheol. Acta **9**, 569 (1970).
[6] S. E. Mall-Gleissle, W. Gleissle, G. H. McKinley, and H. Buggisch, The normal stress behavior of suspensions with viscoelastic matrix fluids, Rheol. Acta **41**, 61 (2001).
[7] I. E. Zarraga, D. A. Hill, and D. T. Leighton, Normal stresses and free surface deformation in concentrated suspensions of non-colloidal spheres in a viscoelastic fluid, J. Rheol. **45**, 1065 (2001).
[8] W. R. Hwang, M. A. Hulsen, H. E. H. Meijer, and T. H. Kwon, Direct simulations of particle suspensions in a viscoelastic fluid in sliding bi-periodic frames, J. Non-Newton. Fluid Mech. **121**, 15 (2004).
[9] Y. Choi, M. A. Hulsen, and H. E. H. Meijer, An extended finite element method for the simulation of particulate viscoelastic flows, J. Non-Newton. Fluid Mech. **165**, 607 (2010).
[10] N. A. Patankar and H. H. Hu, Rheology of a suspension of particles in viscoelastic fluids, J. Non-Newton. Fluid Mech. **96**, 427 (2001).
[11] D. L. Koch and G. Subramanian, The stress in a dilute suspension of spheres suspended in a second-order fluid subject to a linear velocity field, J. Non-Newton. Fluid Mech. **138**, 87 (2006).
[12] D. L. Koch and G. Subramanian, Corrigendum to the stress in a dilute suspension of spheres suspended in a second-order fluid subject to a linear velocity field, J. Non-Newton. Fluid Mech. **153**, 202 (2008).
[13] J. M. Rallison, The stress in a dilute suspension of liquid spheres in a second-order fluid, J. Fluid Mech. **693**, 500 (2012).
[14] A. Einstein, Eine neue bestimmung der molekuldimensionen, Ann. Phys. (Leipzig) **19**, 289 (1906).
[15] E. J. Hinch, An averaged-equation approach to particle interactions in a fluid suspension, J. Fluid Mech. **83**, 695 (1977).
[16] R. G. Larson, *Constitutive Equations for Polymer Melts and Solutions* (Butterworth, Boston, 1988).
[17] J. H. Peery, Fluid mechanics of rigid and deformable particles in shear flows at low Reynolds numbers, Ph.D. thesis, Princeton University, 1966.
[18] F. Greco, G. D'Avino, and P. L. Maffetone, Rheology of a dilute suspension of rigid spheres in a second order fluid, J. Non-Newton. Fluid Mech. **147**, 1 (2007).
[19] K. D. Housiadas and R. I. Tanner, On the rheology of a dilute suspension of rigid spheres in a weakly viscoelastic matrix, J. Non-Newton. Fluid Mech. **162**, 88 (2009).
[20] D. V. Boger, A highly elastic constant-viscosity fluid, J. Non-Newton. Fluid Mech. **3**, 87 (1977).
[21] L. M. Quinzani, D. H. McKinley, R. A. Brown, and R. C. Armstrong, Modeling the rheology of polyisobutylene solutions, J. Rheol. **34**, 705 (1990).
[22] D. M. Binding, D. M. Jones, and K. Walters, The shear and extensional flow properties of M1, J. Non-Newton. Fluid Mech. **35**, 121 (1990).
[23] R. B. Bird, R. C. Armstrong, and O. Hassager, *Dynamics of Polymeric Liquids* (Wiley, New York, 1987), Vol. I.
[24] J. Michele, R. Patzold, and R. Donis, Alignment and aggregation effects in suspensions of spheres in non-Newtonian media, Rheol. Acta **16**, 317 (1977).
[25] R. Scirocco, J. Vermant, and J. Mewis, Effect of the viscoelasticity of the suspending fluid on structure formation in suspensions, J. Non-Newton. Fluid Mech. **117**, 183 (2004).

[26] M. K. Lyon, D. W. Mead, R. E. Elliott, and L. G. Leal, Structure formation in moderately concentrated viscoelastic suspensions in simple shear flow, J. Rheol. **45**, 881 (2001).
[27] D. Won and C. Kim, Alignment and aggregation of spherical particles in viscoelastic fluid under shear flow, J. Non-Newton. Fluid Mech. **117**, 141 (2004).
[28] R. J. Phillips and L. Talini, Chaining of weakly interacting particles suspended in viscoelastic fluids, J. Non-Newton. Fluid Mech. **147**, 175 (2007).
[29] S. Yoon, M. A. Walkley, and O. G. Harlen, Two particle interactions in a confined viscoelastic fluid under shear, J. Non-Newton. Fluid Mech. **185**, 39 (2012).
[30] F. Snijkers, R. Pasquino, and J. Vermant, Hydrodynamic interactions between two equal sized spheres in viscoelastic fluids in shear flow, Langmuir **29**, 5701 (2013).
[31] E. Lauga, Locomotion in complex fluids: Integral theorems, Phys. Fluids **26**, 081902 (2014).
[32] G. K. Batchelor, The stress system in a suspension of force-free particles, J. Fluid Mech. **41**, 545 (1970).
[33] F. Snijkers, G. D'Avino, P. L. Maffettone, F. Greco, M. A. Hulsen, and J. Vermant, Effect of viscoelasticity on the rotation of a sphere in shear flow, J. Non-Newton. Fluid Mech. **166**, 363 (2011).
[34] O. G. Harlen and D. L. Koch, Simple shear flow of a suspension of fibers in a dilute polymer solution at high Deborah number, J. Fluid Mech. **252**, 187 (1993).
[35] G. D'Avino, M. A. Hulsen, F. Snijkers, J. Vermant, F. Greco, and P. L. Maffetone, Rotation of a sphere in a viscoelastic fluid subjected to shear flow. Part I: Simulation results, J. Rheol. **52**, 1331 (2008).
[36] S. Padhy, E. S. G. Shaqfeh, G. Iaccorino, J. F. Morris, and N. Tonmukayakul, Simulations of a sphere sedimenting in a viscoelastic fluid with cross shear flow, J. Non-Newton. Fluid Mech. **197**, 48 (2013).